Disc. 110-S01/From the January-February 2013 *ACI Structural Journal*, p. 3

Ultimate Strength Domain of Reinforced Concrete Sections under Biaxial Bending and Axial Load. Paper by Francesco Vinciprova and Giuseppe Oliveto

Discussion by Phillip J. Thompson

ACI member, Palm Desert, CA

The paper presents a method for the construction of the strength domain of concrete sections that includes a numerical algorithm to integrate the stress components over the cross section based on the integration of the governing equilibrium equations and constitutive laws for the constituent materials.

This discussion suggests an alternative numerical algorithm that could replace that algorithm to greatly enhance the overall method. The alternative algorithm was presented in *Concrete International* in 1995.[48]

A computer program implementing the method could be less complicated and the special needs of the constitutive laws of different materials could be accommodated in separate computer programs for each material, there being a simple standard protocol for input to the main computer program.

In the algorithm, the paper presents the cross section divided into a finite number of trapezoids with bases parallel to the neutral axis and the two oblique sides belonging to its boundary. In a general-purpose computer program, this would be very complicated.

In contrast, with the 1995 algorithm, each part of the boundary is dealt with independently of all the other parts of the boundary. A program implementing the algorithm can simply follow around the boundary.

The paper gives equations for the constitutive laws in Eurocode 2[6] and Eurocode 4[7] and for the softening Kent and Park[37] law, and comments that corresponding results may be easily found for several other common constitutive laws. The inference is that these equations can be included in a computer program that implements the entire method and that that program could be later modified to accommodate other constitutive laws. In contrast, the 1995 algorithm allows for the establishment of a simple protocol to describe constitutive laws so that the main computer program that constructs the strength domain can read the constitutive laws as input data. Other computer programs specific to each material can write that constitutive law data.

In describing the implementation of the method, the paper illustrates that it is assumed that all boundaries of the cross section are straight line segments; if a curved boundary exists, it is assumed that this can be approximated by a polygonal. The 1995 algorithm also uses this assumption.

Further, the 1995 algorithm uses this assumption for the strain-stress relationship in the constitutive law of each material. Curves described by algebraic expressions as are incorporated into some building codes are approximated by a sequence of straight segments, which can be made as close as possible to the given curve as the number of vertices of the approximating segments increases.

Where curves are approximated by straight segments, a strain-stress relationship can be represented in a table of two columns: one column for strain and one for stress, with each line representing a vertex. This is relatively simple and has a clear meaning. Any strain-stress relationship can be represented in this way.

Computer programs to fit a sequence of straight line segments to an algebraic expression such as in the Eurocodes[6,7] or the Kent and Park[37] law can be developed independently of the general-purpose main program. The output from such a code-specific program is a simple strain-stress table. These data can be represented graphically and are amenable to manual checking.

The algorithm presented in the paper can represent certain algebraic expressions exactly—possibly an advantage over the 1995 algorithm. However, these strain-stress relationships are generally only an approximation: they are based on intuition rather than science. The specific algebraic expressions that have been written into the codes typically fit an envisaged computation method rather than a scientific rationale on the properties of the material. Computations using a sequence of straight segments to represent an algebraic expression can satisfy the intent of such codes.

The 1995 algorithm is similar to the algorithm in the paper in that it requires a Cartesian orthogonal reference system 0, *x*, *y* defined such that the x-axis is parallel to the neutral axis.

The partition lines between the trapezoids described in the paper are parallel to the neutral axis. The y-value for each of these is known; being either y_o , y_{c1} or the y-value for a vertex of the polygon.

The 1995 algorithm uses a sequence of y-values each corresponding to a vertex in the strain-stress relationship of the material. An equation derived from Eq. (6) is used

$$y = y_o + \varepsilon/K \tag{26}$$

where ε is the strain at such a vertex.

Each of these y-values is similar to the y_o and the y_{c1} in the paper in that a corresponding strain is known.

By Eq. (9), the paper defines parameters *m* and *q* for each side of the polygon.

The variable *x* does not appear in Eq. (22) through (24), although the *m* and *q* parameters appear many times.

The parameter *m* would present unnecessary problems in a computer program implementing the method because, in the physical model, there are no limits on the value it can take. The paper points out that in the equations to determine *m* and *q*, Eq. (10) requires that the side of the polygon is not parallel to the x-axis—a reference to the same problem.

In contrast, the 1995 algorithm works with the x-values of the points on the perimeter of the polygon. Some of these need to be computed by interpolating between adjacent vertexes of the polygon. The part of the algorithm that determines which vertexes compares the subject y-value with the y-values of the vertexes and ensures the subject y-value is between those of the vertexes. The subject *y* is

never between adjacent vertexes that have the same y-value: there is never a need to compute an x-value on a polygon side that is parallel to the x-axis.

Thus, with the 1995 algorithm, both the x- and y-values are either known or computed for all points on the perimeter where the strain equals the strain at one of the vertexes in the strain-stress relationship of the material.

These points, together with the vertexes of the polygon, divide the perimeter into segments such that within each segment, the perimeter is straight and the stress-strain relationship is linear.

Let n be the total number of such segments and let i identify one segment.

Let subscripts a and b denote the extremities of segment i such that from a to b is clockwise around the polygon.

The strain at each vertex of the polygon can be found by Eq. (6). Thus, the strain is known at all these points and therefore the stress at all the points can be obtained from the strain-stress relationship.

Let σ_a and σ_b represent the stress at the points a and b.

Parameters R_i, S_i, and T_i are defined by the following equations

$$R_i = (y_a - y_b)(2x_a\sigma_a + x_a\sigma_b + x_b\sigma_a + 2x_b\sigma_b)/6 \quad (27)$$

$$S_i = (y_a - y_b)[x_a y_a(3\sigma_a + \sigma_b) + (x_a y_b + x_b y_a)(\sigma_a + \sigma_b) + x_b y_b(3\sigma_b + \sigma_a)]/12 \quad (28)$$

$$T_i = (y_a - y_b) \times [x_a^2(3\sigma_a + \sigma_b) + 2x_a x_b(\sigma_a + \sigma_b) + x_b^2(3\sigma_b + \sigma_a)]/24 \quad (29)$$

These parameters summed around the perimeter of the polygon give, respectively, the axial force N^m in the polygon of the particular material and the moments of that force about the x and y axes, $M^m{}_x$ and $M^m{}_y$.

$$N^m = \sum_{i=1}^{i=n} R_i \quad (30)$$

$$M^m{}_x = \sum_{i=1}^{i=n} S_i \quad (31)$$

$$M^m{}_y = \sum_{i=1}^{i=n} T_i \quad (32)$$

The four terms in the first Eq. (20) that are various summations of N_i^c can be replaced by one term such as N^m.

The four terms in the second Eq. (20) that are various summations of $M_{xi}{}^c$ can be replaced by one term such as $M^m{}_x$.

The four terms in the third Eq. (20) that are various summations of $M_{yi}{}^c$ can be replaced by one term such as $M^m{}_y$.

Also, the terms in Eq. (20) that are summations of N_i^{ss}, $M_{xi}{}^{ss}$, and $M_{yi}{}^{ss}$ can be replaced by terms such as N^m, $M^m{}_x$, and $M^m{}_y$, respectively.

The 1995 algorithm was used in a computer program released in 1986 and was tested against a number of examples available in the literature at that time. It was claimed that this program could work with exactly the same assumptions as the established conventional computation methods to produce exactly the same results. This point was illustrated in most examples. Many examples came from text books such as Park and Paulay,[16] Warner et al.,[49] and Collins.[50] Example 5.8 in Warner et al.[49] included a parabolic strain-stress curve that was represented by 12 straight segments. Several examples in Collins[50] used curved strain-stress relationships.

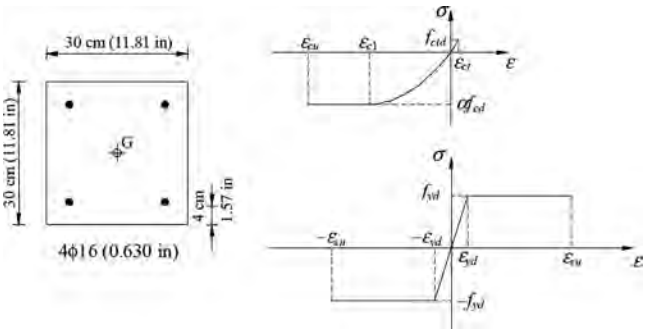

Fig. 13—Reinforced concrete square cross section considered by Thompson.[48]

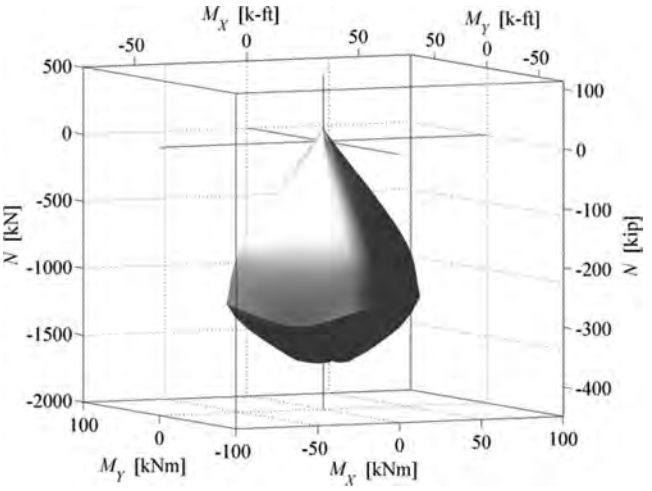

Fig. 14—Three-dimensional uncracked strength domain for reinforced concrete section of Fig. 13.

REFERENCES

48. Thompson, P. J., "A Cross Section Analysis Method for Computer," *Concrete International*, V. 17, No. 12, Dec. 1995, pp. 43-45.

49. Warner, R. F.; Rangan, B. V.; and Hall, A. S., *Reinforced Concrete*, third edition, Longman Cheshire, London, UK, 1989, 553 pp.

50. Collins, M. P., *Prestressed Concrete Structures*, Prentice Hall, Upper Saddle River, NJ, 1991, 766 pp.

AUTHORS' CLOSURE

The authors are happy that their work has raised the interest of the discusser. Unfortunately, at the time they wrote the paper, the authors were not aware of the work by the discusser. The short 1995 paper by Thompson[48] does indeed point out additional applications of the method presented by the authors, such as the construction of a limit domain for the uncracked reinforced concrete cross section. The limit domain for the uncracked reinforced concrete cross section shown in Fig. 1 of Thompson[48] and shown herein in Fig. 13, would look like that shown in Fig. 14. The constitutive law for concrete in compression described by Eq. (12) was used along with a linear behavior for concrete in tension, and the constitutive law for steel given by Eq. (18). The numerical values of the material parameters are specified in Table 1.

The ultimate strength domain for the same cross section is shown in Fig. 15 for comparison. The limit domain for the uncracked cross section of Fig. 14 is contained within

Table 1—Material parameters

Concrete								Steel		
f_{ck}, MPa (ksi)	αf_{cd}, MPa (ksi)	$f_{ctk,0.05}$, MPa (ksi)	f_{ctd}, MPa (ksi)	E_c, GPa (ksi)	$\varepsilon_{ct} \times 10^{-5}$	$\varepsilon_{c1} \times 10^{-3}$	$\varepsilon_{cu} \times 10^{-3}$	f_{yd}, MPa (ksi)	E_s, GPa (ksi)	ε_{su}
30 (4.35)	15.94 (2.31)	2 (0.29)	1.25 (0.18)	32 (4641)	3.90625	–1	–3.5	400 (58.02)	200 (29,000)	0.01

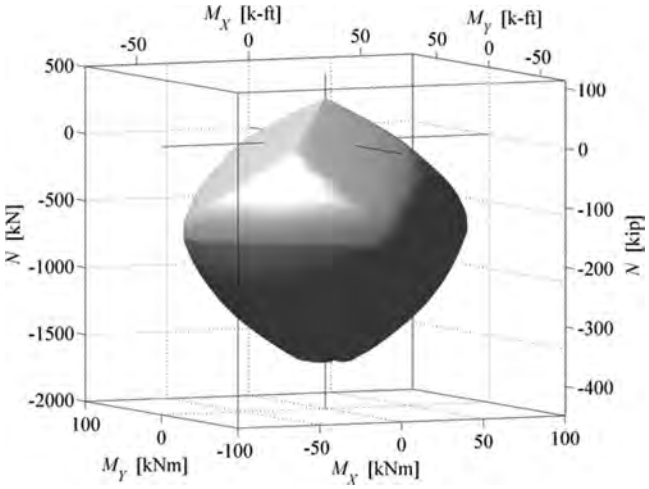

Fig. 15—Three-dimensional ultimate strength domain for reinforced concrete section of Fig. 13.

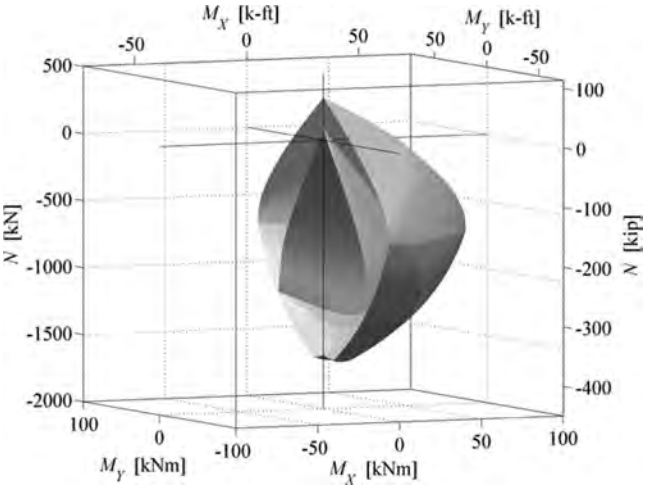

Fig. 17—Three-dimensional uncracked and ultimate strength domain for reinforced concrete section of Fig. 13.

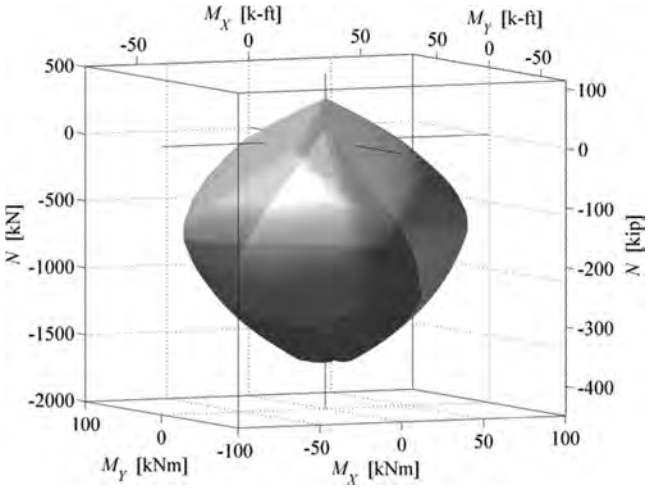

Fig. 16—Three-dimensional uncracked and ultimate strength domain for reinforced concrete section of Fig. 13.

Fig. 18—Original physical model of strength domain by Marín.

the ultimate strength domain of Fig. 15, as seen from direct comparison or by the graphical representation of Fig. 16. An additional comparison is given in Fig. 17, where only half of the two domains considered are shown. It is clear from these figures that the uncracked condition considerably shrinks the strength domain under predominant tension and bending stress resultants, while the two domains are almost coincident under predominant compression states of stress.

The discussion shows that the work has been thoroughly understood, as far as the construction of the stress resultants is concerned, and that the procedure described by Thompson[48] represents an alternative approach that might be appealing to a segment of readers with specific background and taste. The piece-wise linearization of the constitutive laws is an approximation that, in some cases, is unavoidable. However, in most cases it can be avoided, and faster computations and exact results are the obvious outcome. The authors believe that the integration method proposed in the paper is in most cases more efficient than the approximation suggested in the discussion. The differences are only a matter of details and both methods are based on elementary integration formulas. Any particular user is likely to implement the method that is more appealing to his/her taste. Therefore, the authors are grateful to the discusser for recommending his alternative integration method including piece-wise linearization of the constitutive laws as a preliminary step. However, the authors would like to emphasize that the aim of the proposed method was the construction of the "full"-strength domain of the cross section, which does not involve an iterative procedure as

implied in the paper by Thompson[48] and in most of the literature on the subject. Avoiding the iteration procedure was the main motivation for the paper. The authors could find a precursor of the method only in the early work by Marín,[36] who even constructed three-dimensional physical models of the strength domain. Meanwhile, the authors have established a direct contact with Professor Marín and have discovered the existence of fundamental work that can be beneficial to potential users of the method described in the paper under discussion.[51-53] In his work, Marín shows that any polynomial function over a simply or multiply connected cross section of polygonal shape can be integrated in closed form. The work by Marín[36] and the method proposed by Thompson[48] provide alternatives to the approach presented in the paper, which indeed works very well, as shown by the various examples provided. The authors believe that reproduction in Fig. 18 of the original model by Marín is the ideal conclusion to this discussion.

REFERENCES

51. Marín, J., "Computing Unidimensional Normal Stress Resultant," *Journal of the Structural Division*, ASCE, V. 106, No. 1, 1980, pp. 233-245.

52. Marín, J., "Computing Columns, Footings and Gates through Moments of Area," *Computers & Structures*, V. 18, No. 2, 1984, pp. 343-349.

53. Marín, J., "El Cálculo de Integrales Dobles con Momentos de Área," *Boletín Técnico del IMME*, No. 76, 1988, pp. 143-155.

Disc. 110-S05/From the January-February 2013 *ACI Structural Journal*, p. 43

Shear Behavior of Reinforced High-Strength Concrete Beams. Paper by S. V. T. Janaka Perera and Hiroshi Mutsuyoshi

Discussion by Shiming Chen and Jiayang Li

Professor, School of Civil Engineering, Tongji University, Shanghai, China; Research Student, School of Civil Engineering, Tongji University

The use of high-strength concrete (HSC) in the construction industry has increased because of its improved mechanical properties compared to ordinary concrete. One important issue in design consideration for reinforced HSC is the shear resistance of the structural members.[21] Unlike the reinforced normal-strength concrete (NSC), the shear strength of reinforced HSC (RHSC) beams does not increase in the same proportion as the increase in the compressive strength of concrete. The paper provides a group of test data related to the shear behavior of RHSC beams without web reinforcement. The work and the methodology reported would have the positive push and fill the knowledge gap in understanding the behavior of RHSC members in shear. Some detailing needs further discussion and clarification.

HSC is comparatively a brittle material, as the sound matrix of aggregates and cement paste provides a smoother shear failure plane that leads to its abrupt failure. Consequently, the shear strength of HSC does not increase in the same way as its compressive strength. One reason to support the abrupt behavior in shear of HSC is its variation of the fracture surface roughness. Shown in Fig. 8 of the paper, fracture surface roughness is drawn against the compressive strength, and the roughness index R_s of the fracture surface decreases when compressive strength of the concrete specimens increases. It implies that shear failure planes in HSC are smoother than those likely observed in NSC. No direct quantitative expression has been found thus far to link the shear strength and the roughness index R_s of the fracture surface for HSC. In a term of the ductility number (*DN*—the ratio of uniaxial compressive strength to tensile strength of the material), one can find (as shown in Fig. 14) the likely higher strength of concrete is, the higher the *DN* and hence the more brittle the concrete. Figure 14 is drawn based the measurement of specimens reported in the paper. The ductility number of aggregate is between 18 and 22, coinciding with most HSC specimens in the test. In this region, the shear strength of the concrete should remain constant, as was a main conclusion of the research reported in the paper. However, this constant shear strength is not clearly illustrated in the paper. Can the authors comment further on this issue? Besides practice, can the ductility numbers be a design parameter in assessing the shear strength of concrete?

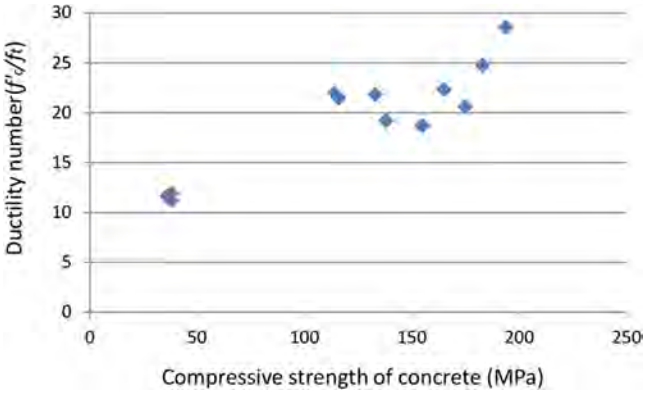

Fig. 14—Ductility number of concrete. (Note: 1 MPa = 145 psi.)

To illustrate the shear strength behavior of concrete, based on the test results given in Table 1, the normalized shear strength of concrete is drawn against the compressive strength in Fig. 15. It appears that the shear strength of concrete does not increase with the compressive strength.

It is known that shear resistance is a factor of the tensile strength of concrete, shear span-depth ratio (a/d), and the tensile reinforcement ratio. In most cases, the tensile strength of concrete and tensile reinforcement ratio has a direct proportionality relation, and a/d has an inverse proportionality relation. In account of these likely influence factors, a shear influencing parameter (SIP) is introduced.[22] The SIP is defined as

$$\text{SIP} = \frac{f_t \rho}{a/d} \tag{9}$$

where a/d is the shear span-depth ratio; and ρ is the tensile reinforcement ratio.

Table 6—Comparison of experimental results with predicted values of shear strength

Specimen	$V_{test}/V_{predict}$*		
	Eq. (10)	Eq. (11)	By MCFT†
NSC40-I	1.17	1.51	1.12
NSC40-II	1.05	1.35	1.21
NSC40-III	0.91	1.18	1.27
HA100-I	1.29	1.63	1.06
HA100-II	1.12	1.42	1.09
HA100-III	0.99	1.26	1.13
HA120	0.94	1.19	1.08
HA160-I	1.21	1.52	0.97
HA160-II	1.00	1.27	0.91
HA160-III	0.85	1.08	0.94
LA120	0.96	1.22	1.02
LA160	0.76	0.96	0.78
Average (all beams)	1.02	1.30	1.05
Standard deviation (all beams)	0.13	0.18	0.13

*V_{test} is experimental shear strength; $V_{predict}$ is predicted shear strength.
†Modified MCFT method.

The normalized shear strength of concrete is drawn against SIP, as shown in Fig. 16. A similar shear performance varying with the shear influencing parameter is found. An approximating curve to evaluate the shear strength of RHSC beams then is developed, which is expressed as follows

$$v_c = 0.0039\text{SIP}^{-0.944} \quad (10)$$

where v_c is shear strength and SIP is shear influencing parameter as expressed in Eq. (10).

The lower-bound fitting curve is expressed as

$$v_c = 0.0034\text{SIP}^{-0.92} \quad (11)$$

The test results compared with predictions based on Eq. (10) and (11) in Table 6. As a comparison, the Modified Compression Field Theory (MCFT) predictions (reducing a_g to zero) are also given in the last column of Table 6.

The results predicted based on the new equations are very promising. The average ratio of the tested-to-predicted shear strength of all beams based on Eq. (11) is 1.02 with a standard deviation of 0.13. Equation (11), based on the lower-bound fitting curve, gives a mean value of 1.30 with a standard deviation of 0.18.

Compared with the MCFT method, the prediction of shear strength of reinforced HSC beams based on Eq. (10) and (11) is much more simple but with almost the same accuracy. The new equations can reflect the shear strength performance in reinforced HSC members.

REFERENCES

21. Russo, G.; Somma, G.; and Angeli, P., "Design Shear Strength Formula for High Strength Concrete Beams," *Materials and Structures*, V. 37, Dec. 2004, pp. 680-688.

22. Sudheer, R. L.; Ramana, R. N. V.; and Gunneswara, R. T. D., "Shear Resistance of High Strength Concrete Beams without Shear Reinforcement," *International Journal of Civil and Structural Engineering*, V. 1, No. 1, 2010, pp. 101-113.

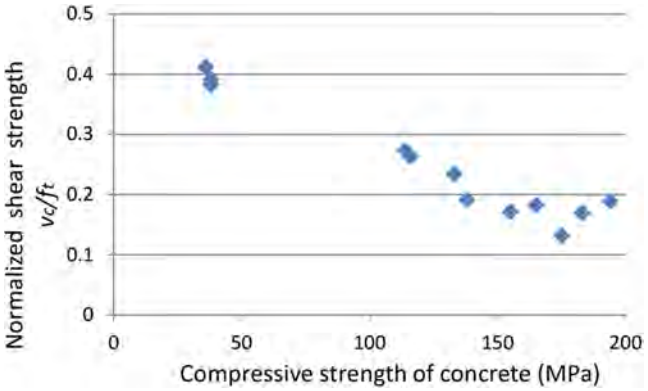

Fig. 15—Behavior of normalized shear strength with compressive strength of concrete. (Note: 1 MPa = 145 psi.)

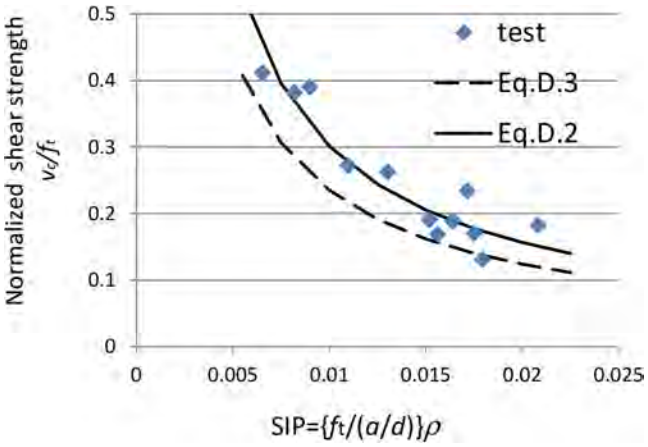

Fig. 16—Behavior of normalized shear strength with shear influencing parameter (SIP).

AUTHORS' CLOSURE

The authors would like to thank the discussers for their interest and discussion related to the paper. The discussers have correctly identified the importance of understanding shear behavior of reinforced high-strength concrete (RHSC) members. The questions and ideas raised in the discussion are addressed herein.

The diagonal cracking shear behavior of RHSC beams without web reinforcement conjunction with ductility numbers (*DN*, the ratio of uniaxial compressive strength to tensile strength) of concrete and aggregate was discussed in the paper. According to the conclusions of the paper, the ductility number of aggregate (*DNA*) relative to that of concrete governs the fracture surface roughness and brittleness. When the *DN* of concrete (*DNC*) is lower than that of aggregate, the shear strength increases with the increase of concrete strength due to the rough fracture surface and increased tensile strength. When the *DN* of the concrete coincides with that of the aggregate, the shear strength remains constant irrespective of concrete strength. However, when the *DNC* is higher than that of the aggregate, shear strength starts to decrease due to smooth fracture surface and high brittleness of the concrete.

The first question was on the constant shear strength region, where the *DN* of the concrete coincides with that of the aggregate. In this region, concrete brittleness is

the same as that of aggregate (*DNC* = *DNA*). The shear resistance of uncracked concrete in the compression zone is dependent on its brittleness.[6] Therefore, the shear resistance of uncracked concrete in the compression zone could be constant irrespective of concrete strength. The fracture surface roughness was slightly higher than that of high-strength concrete (*DNC* > *DNA*) due to aggregate strength anisotropy[17,23] (Fig. 7). Also, concrete tensile strength is higher than that of normal-strength concrete (NSC). Therefore, in this region, the diagonal cracking shear strength stayed constant at the maximum value.

The second and last question is about the applicability of the *DN* as a design parameter in assessing the shear strength of concrete. According to this study, the maximum diagonal cracking shear strength was observed when the *DNC* is equal to the *DNA*. Therefore, optimal concrete compressive strength region for the shear design can be found by considering the *DN* of concrete relative to that of aggregate. That is, by varying the concrete strength from NSC to HSC, the optimal concrete strength region for a particular aggregate type can be found experimentally as presented in this study (Fig. 6 and 8). Therefore, the authors would like to strongly recommend using the *DN* as a shear design parameter. However, further studies on this research area are essential.

The authors appreciate the discussers' observation in predicting normalized shear strength. However, the authors would recommend further studies on the discussers' idea.

REFERENCES

23. Perera, S. V. T. J., "Shear Behavior of RC Members Using High-Strength Concrete," PhD thesis, Department of Civil and Environmental Engineering, Saitama University, Saitama City, Japan, 2011.

Disc. 110-S08/From the January-February 2013 *ACI Structural Journal*, p. 71

Adaptive Stress Field Models: Formulation and Validation. Paper by Miguel S. Lourenço and João F. Almeida.

Discussion by Rafael Alves de Souza

ACI member, Associate Professor, Universidade Estadual de Maringá, Maringá, Brazil

The authors have proposed an extension of the stress-field-based models for the nonlinear analysis of discontinuity regions related to the structural concrete. As mentioned by the authors, this procedure may allow a consistent study of the service behavior of D-regions, usually assumed as a minor issue when using strut-and-tie models or the classic stress field models. Despite the quality of their research, some additional issues should be discussed to clarify some topics and enhance the comprehension of this very interesting paper.

INTRODUCTION

The authors have mentioned that their proposed technique, named Adaptive Stress Field Models, is meant to provide a step forward in the application of stress field models for the analysis and design of structural concrete. To achieve their objective, the configuration of the stress field models is based on the least complementary energy for each load step and includes some concepts related to the Tension Chord Model (Marti et al. 1998). Could the authors explain in more detail the effective advantages of their procedure regarding the other available procedures using the Stress Fields Method?

As mentioned by the authors, several discontinuity regions were analyzed and the structural behavior for these cases were well-simulated. Unfortunately, it is not very clear throughout the paper if the high-quality figures obtained were based on automatic output results or if the figures were later constructed based on the interpretation of some output file containing the results. Could the author better explain the process for constructing their stress field figures?

RESEARCH SIGNIFICANCE

As mentioned by the authors, the application of stress field models in the design process is not fully exploited yet. One reason for this situation is the non-uniqueness of the design models, which raises the discussion of the validity of the models, mainly concerning ductility and service behavior.

In the discusser's opinion, both stress field models and strut-and-tie models are still not deeply used in practice based on the fact that the powerful commercial nonlinear tools available to verify the proposed models usually require the definition of uncountable parameters. In fact, nonlinear analysis of structural concrete based on this kind of powerful package software is far from the reality of the practicing engineer who needs to come up with creative solutions of design in a short period of time. The combination of simple tools as the one proposed by the authors may undoubtedly overcome the application of both stress field models or strut-and-tie models. However, there are still very good and free tools available for the designers, and the authors/readers are encouraged to compare their procedure with the following suggestions.

To visualize the flow of stress inside a complex region, the free software ForcePad (available at http://forcepad.sourceforge.net) may be used, including the possibility of separation of compression and tension stresses for a better visualization of the stress flow. Also, optimization properties are still available that make it very easy to propose strut-and-tie models in a qualitative way. Once the proposed strut-and-tie models have been proposed based on the ForcePad, the free software CAST (available at http://dankuchma.com/stm/CAST) may be applied to check struts, nodes, and design reinforcement. The combination of these two free tools may help the concrete structural designers greatly in the task of designing very complex D-regions.

A more sophisticated way to design using stress fields, also including nonlinear potentialities, is the application of the free software iConc (available at http://i-concrete.epfl.ch/), from which formulation is based on the Modified Compression Field Theory, one of the most advanced techniques for simulating the nonlinear behavior of the structural concrete.

The discusser has the opinion that very safe design may be obtained using all these very simple/free tools and the divulgation of them is fundamental for spreading the design using stress fields or strut-and-tie models. The authors are encouraged to compare their results with the aforementioned tools to develop a tool that can be used in engineering daily practice.

On the other hand, all the aforementioned tools are not able to give the crack width in a way that analytical procedures based on reinforced concrete ties can be applied. In that sense, the authors should be complimented for developing a new tool incorporating at the same time possibilities for optimizing stress fields and to check crack widths. The consolidation of this type of tool may prompt practicing engineers to apply the nonlinear analysis in daily practice.

STRESS FIELD MODELS

In this topic, the authors should have presented the main differences between stress fields and strut-and-tie models, as it could appear that both procedures are the same thing. Strut-and-tie models have gained popularity throughout the years, and perhaps for that reason it is now present in structural codes worldwide.

The stress field models were developed in the 1970s and 1980s in Zurich and Copenhagen, taking as background the Theory of Plasticity. In the same period at Stuttgart, strut-and-tie models were developed in parallel and independently, based mainly on the equilibrium conditions initiated at the beginning of the twentieth century with the introduction of the truss analogy proposed by Ritter and Mörsh. Basically, the Stress Fields Method is a more general solution that may provide different proposals for strut-and-tie models. On the other hand, strut-and-tie models are basically the simplified result of some stress fields and it is not possible to obtain the stress fields from a single strut-and-tie model. The authors are complimented for their effort in divulgating the Stress Fields Method, a very important method that has already been included in the Swiss Structural Code SIA 262.

FORMULATION

In this section, it is not very clear if the proposed model is based on single bars of a truss, or if it is based on a combination of the aforementioned single bars (steel) and two-dimensional elements (concrete), as shown ahead. The authors have mentioned that for truss structures, the application of their methodology is computationally effortless; some given examples (Fig. 2 and 5) also mentioned a truss structure. Could the authors explain how their procedure was implemented?

COMPRESSION STRESS FIELDS

In this section, it was mentioned that the factor η in Eq. (7) is meant to predict the reduction of the concrete strength caused by the presence of transversal strains. However, it was not possible to find the mentioned factor in Eq. (7). Could the authors confirm if the factor η in their proposal is given by $(\alpha\varepsilon_{cc} - \varepsilon_{cc}^2)/(1 + \beta\varepsilon_{cc})$?

Also regarding Eq. (7), the proposal is first based on the parameter f_c', but when defining the parameter E_{c1}, the parameter f_c is now used. As f_c' is adopted in North America and f_c is adopted in Europe and they have different meanings, a clarification of the correct expression would be helpful. Could the authors explain if they have tested different expressions for the factor η and why they did not adopt the classical expression proposed by Vecchio and Collins (1986)?

TENSION STRESS FIELDS

In the discusser's opinion, this section is one of the most important sections of the presented paper, as the authors enhanced the available models implementing concepts based on the Tension Chord Model proposed by Marti et al. (1998). However, Eq. (9) to (12) and Fig. 4 could be better explained, as they were simply included in the paper without explanation. Could the authors better explain at least Fig. 4 in a more detailed way?

The authors have some concern regarding a reliable model for simulating stabilized and nonstabilized cracking, but in the presented examples, this situation is not very clear. Could the authors explain if they have also tested in their examples the model presented in Fig. 4(b)?

It is known that for B-regions (when bending deformation is preponderant), the moment is taken by a couple formed by compression and tensile forces applied at the upper and lower chords. Also, the tensile force in the lower chord (tie) is variable to equilibrate the compressive force in the upper chord (strut). On the other hand, in the D-regions (when shear deformation is preponderant), the force in the tie is usually constant in a way that the model presented in Fig. 4(b) has been applied almost as an unchangeable rule in many research studies. The authors are again complimented for their advance in simulating reinforced concrete ties.

VALIDATION

The validation of the proposed formulation was performed by comparing the obtained numerical results with the test and nonlinear finite element results from package software ATENA. Could the authors briefly discuss the properties of the constitutive model adopted for the nonlinear finite element simulations when using ATENA?

In almost all simulations, the response was quite rigid when compared to their numerical results and test results. Also, in most cases it was not possible to reach the failure load with good precision. Did the authors include all the reinforcement, or did they exclude vertical reinforcement as they did when using their model in some examples?

For the deep beams with top load (Fig. 8 and 9) and for the continuous deep beam (Fig. 12), the vertical reinforcement was not incorporated into the models and still, good results were obtained. One may suppose, based on this fact, that vertical reinforcement has little contribution for the strength of wall structures when, in fact, that is not true. Vertical reinforcement is very important to sew cracks in the direction of the struts due to transversal tensile stress, improving the behavior of a structure as a whole and avoiding fragile failure. For that reason, it is possible to see many cracks parallel to the struts of the example presented in Fig. 12(d)—that is, these cracks are based on the the lack of vertical reinforcement in the example.

The vertical reinforcement excluded in the examples had no influence in the answer, probably due to the fact that the strength of the horizontal ties in the lower chord of the beams is much lower than the capacity of the struts. However, the authors would be prudent to mention that this procedure is just an action for optimizing the construction of the models, and must be conducted with prudence for other situations.

For the example presented in Fig. 10, the vertical reinforcement has been included. Could the authors explain the lack of the vertical and horizontal reinforcement in the last figure of Fig. 10(d)? This figure gave the impression that the figures have been prepared based on some output file and not rendered automatically.

CONCLUSIONS

The authors have presented a very interesting paper and they should be complimented for their effort in divulgating the Stress Fields Method. The proposed technique,

the Adaptive Stress Fields Model, employed the simplifications inherent to the stress field models, given the topologic evolution of the models and the crack widths in the process, helping to check the behavior of complex structures in the service state and ultimate state. The construction of a tool incorporating these two potentialities into a single tool is the main contribution of the authors. The discusser encourages the authors to develop a graphical user interface (if they still do not have one) as well as to simulate other complex examples where nonstabilized cracking is more effective.

Disc. 110-S08/From the January-February 2013 *ACI Structural Journal*, p. 71

Adaptive Stress Field Models: Formulation and Validation. Paper by Miguel S. Lourenço and João F. Almeida

Discussion by Andor Windisch

ACI member, PhD, Karlsfeld, Germany

The authors list in their interesting paper numerous promising notions: Adaptive Stress Field Model (ASFM), adaptive structures concept, model follows energy, form follows energy, and least global energy.

The authors are right: "the cracking pattern is sometimes characterized by a main crack that deeply influences global structural behavior." A typical example is the dapped end shown in Fig. 1. The most important characteristic of this D-region is the inclined crack in the corner. It is not clear how the shaded areas in the graph take this crack into consideration. The anchorage of the ties begins just behind this crack—that is, the fan-shaped struts are nice to see but they do not reflect the real behavior of this beam detail. The failure of such dapped beams occurs due to shortages of the horizontal and vertical reinforcement in the corner. Often, inclined bars are applied there to give the necessary strength to this D-region. It would be helpful if the authors could show how the ASFM overcomes the aforementioned shortages and how it indicates the necessary amount and correct distribution of reinforcement in the corner region.

Dealing with the tension stress fields, the authors write that nonstabilized crack occurs when the length of the tie with constant stresses is not enough to allow the formation of stabilized crack pattern. This is not true. Figure 4(c) is not correct, as well: the crack pattern along a tie with changing tensile stresses has nothing to do with nonstabilized cracking. Please clarify.

The authors validate their models on the deep beams tested by Leonhardt and Walther (1966). The stress field models (Fig. 8(a) and (c)) simulate all horizontal deep beam reinforcements—that is, also the horizontal bars of the "appropriately distributed minimum reinforcement," which always must be applied when strut-and-tie models (STMs) are used at design. It is quite unusual to take into account this reinforcement. The authors need the nodes delivered by these supplementary bars to achieve the possibility of minimizing the complementary energy. Nevertheless, the supplementary bars increase the energy. Neglecting them would let the energy decrease. Why do the authors take them into account? Please clarify.

The ASFMs shown in Fig. 8 raise some interesting questions. The first two models in Fig. 8(a) and (c), respectively, show the uncracked deep beams. Nevertheless, the adaptive stress fields and the STM given there do not reveal the elastic state of stress. Please clarify as to why.

In the dark gray regions, one can guess the course of the struts. In most cases, the struts do not change their direction in the nodes. This should mean that the auxiliary horizontal reinforcing bars are quite stressless. Why undergo the entire calculation procedure?

Deep beam WT2 particularly showed a very pronounced main crack (Fig. 9(a)). The authors correctly mentioned in their paper that, for a reliable model, the consideration of nonstabilized cracking is essential. How was this type of cracking taken into account at the development of the adaptive stress field for WT2? The authors show stabilized crack patterns in the figures. Why?

It might be asked, too, how the global energy dissipated by the numerous thin cracks could approximate the energy of the few wide cracks? Please clarify.

After tedious calculations with the help of their ASFM, the authors make from the deep beams (D-regions) "ordinary" beam sections. Leonhardt and Walther (1966) already concluded in their report that "before cracking the deep beams behave according to the theory of vertical plates assuming homogeneous material. After cracking, however, the actual stresses deviate quite significantly from the theoretical ones. The actual stresses in the reinforcement of the tension chord remain much smaller than the values corresponding to the concrete tensile stresses according to the theory of vertical plates; this is due to the increase in the lever arm of the internal forces." The authors have now demonstrated it after great efforts. As a consequence, how can the deep beam—one of the most characteristic archetypes of the D-regions—be excluded from the exclusive club of discontinuity regions? Do the authors need the nodes delivered by the auxiliary reinforcement to demonstrate this behavior of the deep beams or would the "simple" finite element method reveal the same? Please clarify.

How were the maximum crack widths calculated from the equidistant cracks shown in Fig. 8(b) and (d)? Please clarify.

How was the failure of the deep beams by the ASFMs perceived? Was it the minimal global energy, the yielding of the horizontal reinforcement, or a threshold level of the concrete stress at the support? Please clarify. Note: WT2 failed due to fracture of the tensile reinforcement at middle of the span, and WT3 failed due to overstressing of the concrete above the right support.

How were the shaded areas for the struts as shown in Fig. 8(a) and (c) found?

A comparison of the numerical and test results for the deep beams with suspended loads raises further questions. In their model, the authors take three layers of distributed reinforcement into account. Why? How can a designer make the decision about the number of layers?

According to the force-mean strain curves, ASFM shows WT6 as weaker and WT7 as more rigid than the test curves. The stress field configurations and crack patterns (c) and (e) yielded by the ASFM do not show any similarities to the crack patterns shown in (d) and (f). The shaded patterns here are similar to those shown in Fig. 9(b) and (e). Nevertheless, in the case of WT6 and WT7, the shaded areas cover heavily cracked regions, whereas in the case of WT2 and WT3, the shaded regions are uncracked. It would have been interesting to learn the crack pattern determined with ASFM. The agreement as mentioned by the authors cannot be seen at all. Please clarify. Which kind of failures did ASFM predict?

Opposite to the assertion of the authors, no agreement between the numerical and experimental results in the case of the continuous deep beams can be noticed at all. The shaded areas cover uncracked regions at both ends of DWT2, whereas the shaded regions around the middle support are cracked through and through. Where are the main tension ties above the central support according to the ASFM? Are the tensile stress distributions similar to those attributed to "deep beams" or to "continuous beams"? As shown in Fig. 12(c), in DWT2, the tensile reinforcement above the central support was placed in the lower half of the depth. The shaded areas—that is, the flow of forces—did not show any reference to these ties. Are these reinforcing bars in tension or in compression? At which position should the tension reinforcing bars be placed above the central support? The flow of forces provided by the ASFM does not present the structural behavior at all. Which kind of failure did ASFM predict?

At dimensioning, the designer needs the inner lever arm for calculation of the load-bearing capacity and the steel strain for the crack control. How does the ASFM assist the designer at solving these two everyday questions? Please clarify.

The authors are encouraged to improve their model so that it becomes a legitimate support for the engineer. For the time being, the model cannot be considered validated.

AUTHORS' CLOSURE

Closure to discussion by Souza

The authors kindly appreciate the comments and the discussion provided by Souza and his interest in the paper. Detailed replies to his questions, by section heading, are presented as follows:

- *Introduction*—Unlike other methodologies, Adaptive Stress Field Models intend to set a suitable stress field model and then select the appropriate variables that will be adjusted: model geometry, forces, or both. This procedure allows the engineer to clearly understand behavior of the structure before starting analysis—an essential guideline for a critical evaluation of the results. Furthermore, the graphical interaction provides a valuable tool for understanding structural behavior and correcting possible inaccuracies of the model.
- *Introduction*—The field widths are semi-automatically entered in the calculation and the output is, essentially, the model resultants geometry together with the previously inputted field widths. However, the final drawings are adjusted manually. The authors are now trying to develop an automatic tool to draw stress fields.
- *Research significance*—The authors appreciate the comments in this chapter of the discussion. The main advantages of the presented methodology when compared with other automatic tools were well explained. A final comment should be given to apply this methodology: the user must set an initial stress field model—that is, the intention was not to provide a guidance tool for developing strut-and-tie models, but a methodology to assess strut-and-tie models.
- *Stress field models*—The authors used the term "stress field models" whenever the field widths are computed and may be used for analysis procedures. The term "strut-and-tie model" was used to refer to the resultant model, where only equilibrium conditions may be applied to compute the resultant forces. The authors are aware that both terms refer to the same; however, to extend the concept to evaluate structural behavior, it is necessary to know the field widths.
- *Formulation*—The forces in the bars are calculated according to equilibrium of single bar models. Knowing the resultant forces and the element widths, it is possible to calculate the elements stress state as presented in the sections "Compression stress fields" and "Tension stress fields". Applying the mechanical proprieties of the materials, strains are calculated and therefore are complementary energy of each element.
- *Compression stress fields*—The factor

$$\eta(\varepsilon_1) = \frac{f_c'}{f_c} = \frac{1}{0.8 + 0.34\varepsilon_1 / \varepsilon_{c1}}$$

depends on the transversal tensile strains and the authors apologize for not defining it explicitly.

- *Tension stress fields*—Figure 4 shows the stress and strain state in a reinforced concrete tie. Knowing the axial force in the element, the concrete and steel stresses are calculated following the principles of the Tension Chord Model. With the materials' constitutive relationships it is possible to calculate crack widths, strains, total elongation, and mean strains. The main goal is to achieve an N-ε_m law to compute the complementary energy of a reinforced concrete tie. It was possible to apply a common constitutive relationship as presented in, for example, CEB-FIP MC 90 (1993); however, the authors intended to simulate the situations of nonstabilized cracking. This was achieved by applying Tension Chord Model concept assuming that the reinforced concrete tie has variable axial force (refer to Fig. 4(c)), providing different N-ε_m behavior (refer to Fig. 4(d)).
- *Validation*—The constitutive relationships adopted in the nonlinear finite element model were: concrete—Poisson coefficient of 0.2; tension stiffening function—exponential; fracture energy—0.0000294 × f_c; cracking model—crack rotating; compression strain associated to f_c—(ε_c = –0.0022); compression strength reduction due to cracking—0.8; shear factor r_g—variable; tension/compression interaction—Hyperbole A; steel—bilinear with hardening after yielding; bond—Bigaj (Fig. 13); calculation method—arc-length.
- *Validation*—In fact, the vertical reinforcement efficiently controls crack width avoiding fragile failure. The compression reduction due to transversal tensile strains is less important due to this reinforcement. However, with a simple calculation and excluding the node regions, the compression stresses are relatively small within the deep beams, and thus the effect of transversal strains in the compression strength does not lead to much difference in the global behavior. For

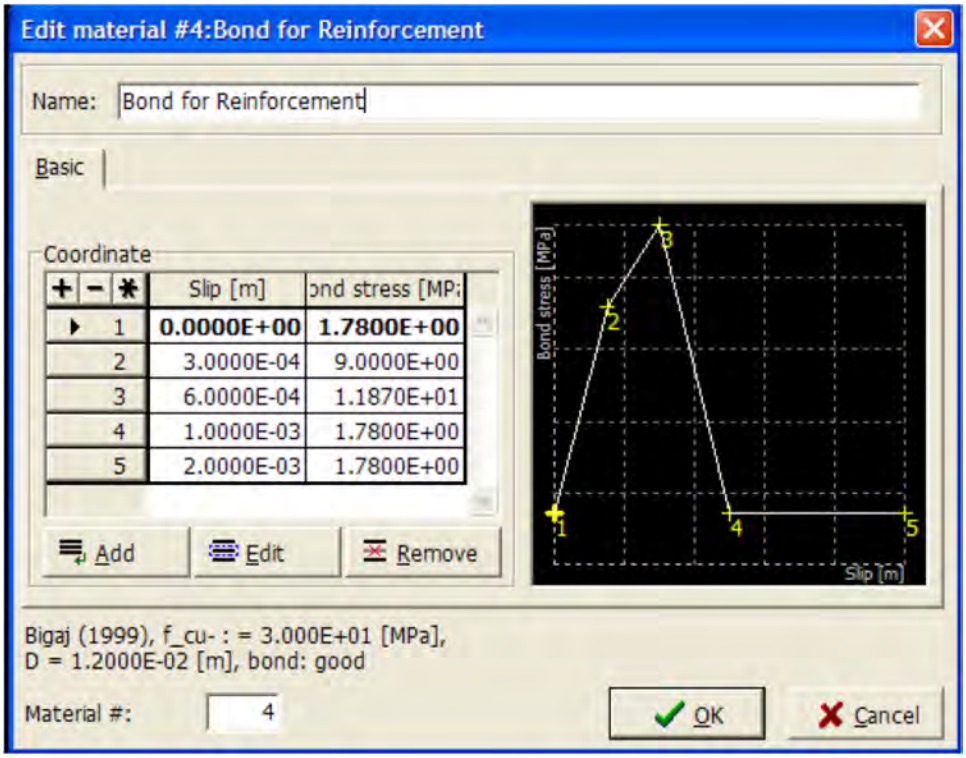

Fig. 13—Bond law used in finite element program ATENA.

that reason, the authors choose to disregard the vertical reinforcement. This was a simplification that may not be applicable in other situations. The authors mention this effect at the Conclusions section of Lourenço and Almeida (2013): "a more detailed analysis should be performed when important compressive stresses cross diagonal ties with significant transverse strains induced."

- *Validation*—In fact, the horizontal and vertical thicker lines are missing in Fig. 10(d), but they were considered in the analysis.
- *Conclusions*—The authors are now trying to develop a more "user-friendly" tool and also applying the Adaptive Stress Field Model concept to reversal loading.

REFERENCES

Lourenço, M., and Almeida, J., 2013, "Adaptive Stress Field Models: Assessment of Design Models," *ACI Structural Journal*, V. 110, No. 1, Jan.-Feb., pp. 83-93.

Closure to discussion by Windisch

The authors kindly appreciate the comments and the discussion provided by the discusser and his interest in the paper. In the following, detailed replies to his questions are presented:

- If no inclined reinforcement is adopted at the dapped beam, the stress field presented in Fig. 1 trustingly represents the load path at ultimate limit state. In Lourenço and Almeida (2013), the authors discuss the importance of inclined reinforcement in a dapped end beam. In cases with high bending moments and/or shear forces, inclined reinforcement is required to effectively control the corner crack. In the particular case of the model presented in Fig. 1, the inclined crack at the corner may be derived by the bidirectional tension stress state represented by the horizontal and vertical ties. Furthermore, as mentioned in the paper, the stress field models are recognized by the valuable information concerning the anchorage length and node region detailing.
- The authors refer to nonstabilized cracking for cases where a main crack occurs in the region and the behavior is mainly influenced by the continuous opening of the main crack. The authors had no intention to mislead the idea of nonstabilized cracking with crack formation phase. The reinforced concrete tie represented in Fig. 4(c) and the "mean behavior" at Fig. 4(d) intend to simulate situations characterized by a main crack. In fact, a stiffer behavior is obtained for this kind of tie and the used energetic criteria lead to a model adjustment that increases the forces in these ties, simulating well the effect of a main crack.
- For discussion on deep beams, the following comments are presented:
  - The consideration of the horizontal bars is essential to predict the gradual increase of the inner lever arm. Otherwise, if only the main reinforcement is considered, a sudden increase of inner lever arm is obtained immediately after cracking of the main reinforcement.
  - The stress field model shown in Fig. 8(a), before cracking (loads 50 to 150 kN [11.24 to 33.72 kip]), model geometry provides the elastic inner lever arm of a deep beam. However, because the ties are placed according to reinforcement layout, elastic trajectories are not explicitly represented. This will slightly compromise the behavior before cracking; however, it is most suitable after cracking, in which its prediction is the main goal of the analysis.
  - The slight changes in the inclination of the struts may not be visible but they exist. This aspect is essential for predicting the forces in the horizontal ties.

- The main crack observed occurred after yielding of the reinforcement and just before deep beam failure (refer to Fig. 8(b), Load versus Maximum Crack Width test diagram). The crack layout is illustrative and does not intend to reproduce the right crack width and crack spacing.
- The presented technique may be an alternative to the finite element method. However, the authors considered that in the first steps of this new methodology, it should be applied for the assessment of strut-and-tie models. The sophisticated nonlinear analyses provided nowadays are reserved for a few researchers and hardly used by designers. Furthermore, it disregards the main objective—to provide guidance for the designers. It is expected that an experienced user of nonlinear finite element programs can provide better results of a specific region than the proposed technique. The main question is: Is such sophistication necessary? Is it possible to develop a new and simpler tool that can easily provide guidance for the designers? Stress fields are first defined as a reproduction of discontinuous compression and tension fields due to the load path deviation for any geometric and static conditions. Rather than a formulation based on abstract physical quantities, a clear physical meaning is envisaged through the visualization of the flow of forces. The Adaptive Stress Field Model (ASFM) is based on a set of adequate simplifications but does not disregard the main physical phenomena of structural concrete regions and, moreover, provides an unprecedented awareness of the structural behavior, which is essential for any researcher or designer. A key phrase may be applied: Think, judge, and feel the structural behavior before analyzing.
- The crack widths are calculated according to the Tension Chord Model concept.
- Both deep beam failures were due to node's compression. In the ASFM it was established the maximum compression at node region, and the load increment stops whenever that limit is reached.
- The strut widths were obtained according to the common equilibrium and boundary conditions for developing stress fields.

- Concerning the deep beams with indirect loads, the following comments are presented:
  - The number of layers of reinforcement must be selected wisely before starting the analysis. The top layers of reinforcement are with very low stresses, as it is possible to see from the strut geometry through the loading process and thus they were disregarded.
  - The shaded areas represent the strut widths; however, there are ties anchoring at that region, providing a biaxial stress state in the shaded area that lead to cracks. It is clear in Fig. 11(c) to (f) that the WT6 inner lever arm almost reached the effective height of the deep beam, which is not evident in deep beam WT7.
  - Both deep beams failures were due to node compression.
- For the continuous deep beam test comparison, the following comments are presented:
  - The ASFM steel stresses obtained agreed well with the test, especially regarding the bottom main reinforcement. Note that the test steel stresses were measured by glued gauges at reinforcement and the analytical analysis did not include the thickness enlargement over the support. These aspects could slightly compromise the final results comparison; however, the main behavior is assumed to be well-simulated.
  - The ASFM main support ties were placed where the main reinforcement is provided, and the tension stresses are presented in Fig. 12(b). These bars are always in tension along the loading process.
  - After cracking, the tensile stresses do not behave like "deep beams," but do not reach "continuous beams" behavior. It is observed an increase of the "support inner lever arm" but did not reach the full height of the deep beam.
  - In Lourenço and Almeida (2013), the reinforcement position above the central support is discussed, analyzed, and assessed. In fact, the presented methodology was mainly applied for assessment of strut-and-tie models to solve the main designer questions when applying these models.
  - The authors considered that the main behavior of the continuous deep beam was well-simulated besides slight differences in results.
- The authors presented a new methodology for analyzing D-regions' structural concrete behavior. The technique provides an excellent awareness of the flow of forces during the loading process and also provides the crack widths. This kind of tool allows a check of complex regions at service loads and ultimate state. The methodology was validated in other D-regions that were not presented in the current paper, and the main structural behavior was always well-simulated. In fact, the authors believe that other methods may retrieve similar results; however, the main intention was to follow consistently the stress field method, which is considered to be the only way to really assess the design with strut-and-tie models.

Adaptive Stress Field Models: Assessment of Design Models. Paper by Miguel S. Lourenço and João F. Almeida

Discussion by Andor Windisch

ACI member, PhD, Karlsfeld, Germany

In the Introduction, the authors refer to the "general and simplified energetic criteria mentioned by Schlaich et al. (1987)." These criteria were never proven. Further on, they state that "an appropriately distributed minimum reinforcement shall be used where no main reinforcement is required." Nevertheless, in Lourenço et al. (2013), the horizontal bars of this minimum reinforcement were involved in the Adaptive Stress Field Model (ASFM) as active ties. What is now true? Please clarify.

For both design strut-and-tie models for pier of viaduct (Fig. 1(a)), the authors choose the inner lever arms to 0.7*L*. This value contradicts the research of Lourenço at al. (2013) in the same journal: the deep beams in that study behaved like B-regions; hence, the inner lever arm could be chosen to 0.9*L* or even more. Please clarify.

From the two deep beams with top loads referred to in this paper, Fig. 2 shows the deep beam with the stronger reinforcement. In the ASFM, both the main and the distributed reinforcement are simulated. This represents two contradictions: 1) the additional minimum web reinforcement is placed "to equilibrate a significant fraction of the concrete tensile strength that overcomes locally after cracking" and not to contribute to the calculated load-bearing capacity; and 2) the energy spent by this additional reinforcement unnecessarily lets the global energy level of the model increase, whereas it should be minimum. Please clarify. The inner lever arm variation shown in Fig. 2(e) reveals that to fulfil the serviceability limit state conditions, the elastic-based strut-and-tie model should be applied.

The conclusions with reference to the deep beam with A_s = 306 mm^2 (0.474 in.^{2}) do not refer to any test of Leonhardt and Walther (1966), where the weaker reinforcement was A_s = 214 mm^2 (0.331 in.^{2}). In the latter case, a very pronounced crack developed in the deep beam. This contradicts the proposal of the authors because the designer has no freedom to choose the design strut-and-tie model: he is well advised to adhere to the elastic-based model.

The models for the deep beams with suspended loads and the conclusions cannot be validated with Leonhardt tests, as none of the tested models had the main reinforcement as referred to in Fig. 3.

The tests of Sahoo et al. (2012) with the model of Schlaich et al. (1987) revealed that this deep beam with opening does not behave like a dapped end but needs a continuous tie between the two supports. The first cracks occurred under the opening; hence, without a continuous tie, the "column" over Support A would immediately fail and the deep beam would "fall to its knees."

A shortcoming of the paper was that the three design strut-and-tie models shown in Fig. 7 do not resolve lingering questions for designers: which percentage of the total vertical load shall be equilibrated by an inclined reinforcement and how much orthogonal reinforcement shall be applied if no inclined reinforcement is desired? How can the ASFM help the designers? What was the reason to show these quite well-known, but non-validated, models? Comparing the reinforcement patterns shown in Fig. 7, large differences can be detected (which contradict the minimum energy concepts). Table 1 compares the reinforcement patterns showing the relevant cross-sectional areas multiplied with the bar length shown in the side views.

Table 1—Comparison of amounts of reinforcement in dapped-end models

Models	Dapped-end horizontal reinforcement, mm^3	Inclined reinforcement, mm^3	Vertical reinforcement, mm^3	Stirrups, mm^3	Total, mm^3
(b)	460	3700	510	770	5440
(c)	920	2460	860	1665	5905
(d)	1640	615	1825	2625	6705
(d)/(b)	3.6	0.17	3.6	3.4	1.2

Note: 1 mm^3 = 6.1 × 10^{-5} in.^{3}.

Significant differences can be detected:

- The amounts of the dapped end horizontal reinforcement of the vertical reinforcement and that of stirrups vary, 1:3.6;
- The amount of the inclined reinforcement varies, 6:1; and
- The total values increase moderately; approximately 25%.

A validation should have been indispensable. Please clarify. The authors are encouraged to improve their model to provide essential guidance to the designers.

REFERENCES

Lourenço, M., and Almeida, J., 2013, "Adaptive Stress Field Models: Formulation and Validation," *ACI Structural Journal*, V. 110, No. 1, Jan.-Feb., pp. 71-81.

Sahoo, D.; Flores, C.; and Chao, S., 2012, "Behavior of Steel Fiber-Reinforced Concrete Deep Beams with Large Openings," *ACI Structural Journal*, V. 109, No. 2, Mar.-Apr., pp. 193-203.

AUTHORS' CLOSURE

The authors thank the discusser for his interest in the paper. Detailed replies to his questions are given in the following:

The general Schlaich et al. (1987) criterion is a simplified indication, but very useful in practice. It should be noted that sometimes this criterion cannot be applied without any other further analysis. Applying the simplified energetic criteria to deep beam models may lead to the assumption that the model that leads to the less main reinforcement is the most adequate. This would be achieved by exploiting the full height of the deep beam for the inner lever arm. However, in these cases, the computation of the compression stress fields' energy is essential for a correct judgment of the strut-and-tie model for the design. This may avoid a deficient service behavior, as is well-explained in the discussed paper, especially for continuous deep beams and deep beams with suspended loads.

A good engineering approach requires the adoption of "an appropriately distributed minimum reinforcement," which should also prevent premature failures at the cracking load.

As is usual in reinforced concrete structures, such reinforcement, although frequently neglected in practice, can slightly increase the ultimate load of the structure. In the mentioned example, Lourenço and Almeida (2013) address the model validation by comparison with experimental results and, thus, it was considered relevant to involve the minimum reinforcement. It does not mean that the designer needs to regard the minimum reinforcement in the strut-and-tie model for the design of a specific region.

For the pier of the viaduct presented in Fig. 1(a), the main problem would certainly not be the reduction of steel reinforcement. As was pointed out, inner lever arms of approximately 0.7*L* indirectly ensure an appropriate service performance; on the other hand, the assessment of models at the service load level has shown that quite large deviations from the elastic solution can be tolerated without greatly affecting the service behavior.

In fact, as the discusser may have noticed in Fig. 2(f), despite such important internal redistributions observed, the steel stresses between 150 and 250 MPa (21.8 and 36.3 ksi) and crack widths at the service load level remained at quite appropriate levels.

In the presented assessment studies, the adopted steel reinforcement amounts do not refer to Leonhardt and Walther (1966) tests. The main objective is to discuss within which limits the designer can choose the model, preventing deficient service behavior and/or premature failure. The analyzed models are representative of several discontinuity regions, simulating the general model of a particular discontinuity region or possibly be included in more complex models. For this reason, the proposed indications may provide guidance for the proper design and detailing of most of the structural concrete regions.

The deep beam with the opening was not analyzed in the paper. It intends to illustrate a dapped-end beam model. Concerning the well-known Schlaich et al. (1987) model, further knowledge is given in the paper of Breña and Morrison (2007).

Concerning re-entrant corner models (Fig. 7 and 8), it is clearly pointed out that inclined reinforcement must be designed to equilibrate more than 50% of the vertical load, as suggested in FIP Recommendations (1999); in fact, referring to service behavior, the stress redistribution that occurred immediately after cracking kept steel stresses at both orthogonal and inclined reinforcements at appropriate levels, suggesting low-to-moderate crack widths.

The mentioned "contradiction" and "differences" referred to by the discusser concerning the dapped-end beam model probably results from a misunderstanding. The amounts of reinforcement presented in Table 1 are only comparable for the total reinforcement. The remaining ratios are pointless. The models that provide better behavior at service loads are (b) and (c) models, which have less "total reinforcement." Indeed, model (b) gives a slightly improved behavior (less steel stresses at service loads) than model (c), which is in accordance with the simplified energetic criteria proposed by Schlaich et al. (1987).

The Adaptive Stress Field Model (ASFM) extends the application of stress-field-based models for the nonlinear analysis of structural concrete discontinuity regions, allowing a consistent study of service behavior and ductility aspects. It is an alternative to nonlinear finite element analysis. More refinements will be performed but, in the authors' opinion, ASFM is presently an excellent approach to address the study of the model's assessment topics.

REFERENCES

Breña, S. F., and Morrison, M. C., 2007, "Factors Affecting Strength of Elements Designed Using Strut-and-Tie Models," *ACI Structural Journal*, V. 104, No. 3, May-June, pp. 267-277.

Lourenço, M., 2010, "Adaptive Stress Field Models for Structural Concrete," PhD dissertation, Instituto Superior Técnico, Lisbon, Portugal, Feb.

Ruiz, M. F., and Muttoni, A., 2007, "On Development of Suitable Stress Fields for Structural Concrete," *ACI Structural Journal*, V. 104, No. 4, July-Aug., pp. 495-502.

Disc. 110-S13/From the January-February 2013 *ACI Structural Journal*, p. 127

Unified Calculation Method for Symmetrically Reinforced Concrete Section Subjected to Combined Loading. Paper by Liang Huang, Yiqiu Lu, and Chuxian Shi

Discussion by Jian Yuan

Lecturer, School of Civil Engineering and Mechanics, Central South University of Forestry & Technology, Changsha, China

Based on bending-torsion, shear-torsion, and bending-axial compression interactions in bridge connections, a unified formula for calculating the ultimate state of reinforced concrete members was obtained, and interaction equations of various types were deduced by the authors. Similar topics were studied before, and it is interesting that such studies are extended to all combined loading conditions in this paper. However, some findings are still questionable and are worthy of further discussion.

The experimental data of Mattock and Wang[31] were cited by the authors to determine the coefficients of Eq. (23) to obtain Eq. (24). The shear-bending interaction was quantitatively described by Eq. (24) in this paper, but the scopes of application and limiting conditions for Eq. (24) were not given.

The definition of shear-bending interaction seems ambiguous in this paper. Moreover, it is not based on any mechanical analysis. As is known to all, when members subjected to combined loading of bending, shear, and torsion, due to the spatial characteristics of torsional failure, the longitudinal reinforcement and stirrups resist torque together. Meanwhile, the longitudinal reinforcement resists bending moment and the stirrups resist shear force, respectively. Because bending moment and shear force are related by torque, will it still exist if there is no torque? According to the definition of the bending-torsion interaction for symmetrically reinforced sections, the torsional capacity is reduced because of the effect of bending moment, and the flexural capacity is also affected by the existence of torque. Nevertheless, the inter-

Table 11—Comparison of actual results and shear-bending interaction formula

Specimen	V_{exp}/V_0	M_{exp}/M_0	Value of Eq. (24)
Mattock and Wang[31] average = 1.49			
C205-D10	1.779	0.769	1.560
C205-D20	1.570	0.767	1.383
C210-D0A	1.475	0.956	1.500
C210-S0	1.686	0.980	1.691
C305-D0	1.360	0.885	1.348
C310-D10	1.128	1.104	1.422
C310-D20	1.188	1.162	1.515

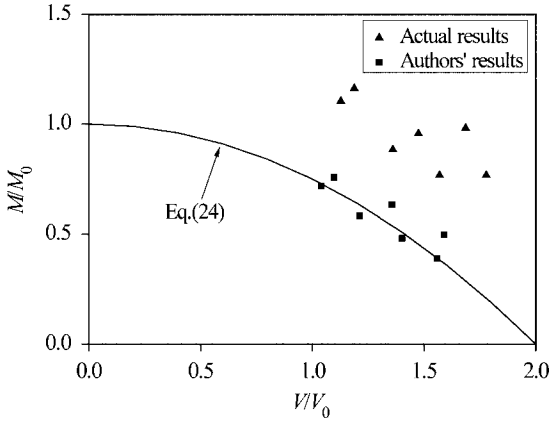

Fig. 9—Comparison between the authors' results and actual results.

Table 12—Actual section details and results of test beams used in Table 11

Beam No.	b_w, mm	h, mm	d, mm	A_s, mm^2	A_s', mm^2	Diameter, m	s, mm	f_y, N/mm^2	f_y', N/mm^2	f_{yt}^*, N/mm^2	f_c', N/mm^2	V_{exp}, kN	M_{exp}, kN.m
C205-D10	150	350	315	1232	157	6	160	361	353	354	23.2	137.4	86.6
C205-D20	150	350	315	982	157	6	160	387	353	354	24.3	122.6	77.3
C210-D0A	150	350	315	1232	157	6	80	361	353	354	27.2	176.6	111.3
C210-S0	150	350	315	1232	1232	6	80	361	361	354	23.0	196.2	123.6
C305-D0	150	350	315	1232	157	6	160	361	353	354	26.0	108.0	102.1
C310-D10	150	350	315	1232	157	6	80	360	353	354	24.3	132.5	125.2
C310-D20	150	350	315	1232	157	6	80	360	353	354	24.5	139.8	132.1

*f_{yt} is yield strength of transverse reinforcement.
Notes: 1 mm = 0.0394 in.; 1 mm^2 = 1.552 × 10^{-3} in.^{2}; 1 N/mm^2 = 145 psi; 1 kN = 0.225 kip; 1 kN.m = 8.87 kip-in.

action proposed to evaluate the influence of bending moment on shear failure still seems questionable.

Kani's[37] "valley of diagonal failure" indicates that the shear strength varies non-monotonically with shear span-depth ratio. The relation between the shear-bending interaction proposed by this paper and the shear capacity affected by shear span-depth ratio is somewhat elusive. In terms of mechanism, how is the shear capacity of beams with web reinforcement related to bending moment?

As for uniform cantilever beams without web reinforcement under a vertical concentrated load at the free end, the flexural capacity depends entirely on the amount of longitudinal reinforcement and the relative depth of compressive area. The increasing stirrups will not have any effect on flexural capacity, but can resist additional shear force.

Provided that simply supported beams are subjected to vertical loads, no matter how the span varies, maximum shear force and zero bending moment will occur simultaneously in the support sections. According to Eq. (24), if M = 0, the value of V will always equal to $2V_0$, which is obviously unreasonable.

Obvious mistakes exist in these data of Tables 1 and 2 of the original paper. In accordance with the experimental data of Mattock and Wang,[31] relevant results are recalculated by the discusser (the results calculated by Russo[38] are consistent with the discusser's). The values of V_{exp}/V_0 and M_{exp}/M_0, by means of Eq. (14), (15), (20), and (21) provided by this paper or its errata (the relevant requirements of ACI 318-05[2] are also used as a reference) are reported in Table 11. Actual section details and results of test beams are listed in Table 12. A comparison between the authors' results and actual results is shown in Fig. 9.

From Table 11 and Fig. 9, it can be concluded that the actual results are inconsistent with the authors', and the behavior of shear-bending members does not agree with Eq. (24). The mean of the experimental data of Eq. (24) is 1.49 rather than 1.03, which implies that Eq. (24) is meaningless. The reason for this is that the original test data have been modified by the authors, which is difficult for the discusser to understand.

From Table 12, it can be seen that only Beam C210-S0 is symmetrically reinforced. Notwithstanding this, all the A_s' of other six beams have been changed to be close to A_s in this paper (refer to Table 1).

In the study of shear-bending-axial compression interaction, Eq. (28) was also calibrated by using the experimental data of Mattock and Wang,[31] but A_s' = 157 mm^2 (0.24 in.^{2}) was mistakenly replaced by A_s' = 1570 mm^2 (2.4 in.^{2}) in Table 3 of the original paper. According to the actual experimental data given by Mattock and Wang[31]and these formulas provided by this paper, the ratio of the experimental results to the calculated value of Eq. (29) should have a mean of 1.46 rather than 1.14, which is the value calculated by the authors. In addition, it is incomprehensible to the discusser that four simple span test specimens with symmetrically reinforced sections were not quoted by the authors.

The unified calculation method proposed by this paper is for symmetrically reinforced sections; however, some other

specimens with asymmetrically reinforced sections (refer to Tables 4 and 6 of the original paper) have also been quoted.

REFERENCES

37. Kani, G. N. J., "Basic Facts Concerning Shear Failure," *ACI Journal*, V. 63, No. 6, June 1966, pp. 675-692.

38. Russo, G., and Puleri, G., "Stirrup Effectiveness in Reinforced Concrete Beams under Flexure and Shear," *ACI Structural Journal*, V. 94, No. 3, May-June 1997, pp. 227-238.

AUTHORS' CLOSURE

The authors are grateful to the discusser for his interest and perspective related to the paper. Detailed replies to his questions and comments are given herein.

Bending-shear interaction

In this paper, the main objective was to propose a unified equation to calculate the strength of reinforced concrete members, including the interaction between bending, shear, torsion, and axial compression. Different interactions between structural actions can be deduced directly from the proposed formula. The parameters of different interaction formulas are determined using experimental data. The questions proposed in the discussion are all related to bending-shear interaction, which is only one type of interaction. However, the comments and questions proposed by the discusser are valuable to the bending-shear interaction part.

The bending-shear interaction formula (Eq. (24)) was derived from test data. Its application and limitations were not researched as part of this study. More experimental data should be compared with Eq. (23) to verify the formula, and further research regarding its application and limitations is required.

In regards to the discusser's point about bending-shear interaction, the definition of interaction used in this paper should be clarified. It was defined that the capacity of a member will be influenced by the interaction of different structural actions on the member. No attempt was made to study the influence of reinforcement to the force capacity. For bending-shear interaction, bending capacity will be influenced by shear force and shear capacity will be influenced by bending moment. This can be verified using the interaction formula in Hsu and Mo's[39] book, *Unified Theory of Concrete Structures*, the interaction diagram of Vecchio and Collins,[11] and the interaction diagram drawn by Bentz's[12] software Response-2000. From their interaction formulas or diagrams, even when torsional forces are not applied to the member, the shear capacity will be influenced by the magnitude of bending moment, indicating that there is bending-shear interaction. Moreover, in various codes and standards, the aspect ratio $M/(Vd)$, which is an index for considering bending-shear interaction for the shear capacity, should be considered in the shear strength formula. This also indicates that bending-shear interaction exists.

In the shear capacity formula, aspect ratio is included for considering its effect to shear strength. In fact, aspect ratio is only an index that considers bending-shear interaction for the shear capacity of reinforced concrete members. In this research, although aspect ratio is not included in Eq. (24), the bending-shear interaction has been considered. Equation (24) and the aspect ratio are two different ways to consider bending-shear interaction. This study used another approach to consider bending-shear interaction. As long as Eq. (24) can fit into experimental results well with a small coefficient of variation, it reflects bending-shear interaction well.

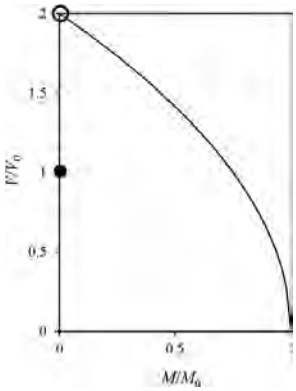

Fig. 10—Bending-shear interaction curve.

The discusser questioned the effectiveness of shear reinforcement to flexural capacity. As stated before, the definition of interaction is that the capacity of a member will be influenced by the interaction of different structural actions on the member. The research did not attempt to investigate the influence of shear reinforcement on bending moment. The authors agree that shear reinforcement has little influence on flexural capacity, but the authors believe that bending-shear interaction exists in the bending-shear components.

The discusser raised the question that if $M = 0$, the value of V will always be equal to $2V_0$, which the discusser regarded as unreasonable. It is true that the bending-shear interaction formula cannot satisfy pure shear force. To solve this problem, the boundary of the bending-shear interaction formula was limited in the paper. As shown in Table 8, for pure shear force, the three parameters α_1, α_2, and α_3 are all equal to 1, which means $V = V_0$. The pure shear and bending-shear interaction is shown in Fig 10. The shear strength will not be equal to $2V_0$, but V/V_0 will be close to 2 when M/M_0 is small. From Fig. 9 and Table 11, in which the discusser showed the experimental comparison result, V/V_0 indeed can get very close to 2, indicating that the shear strength in the bending-shear interaction equation is not very conservative. The comments proposed by the discusser are very valuable to further research to make the bending-shear interaction fit the experimental data better.

Error in experimental data

The authors acknowledge the error that occurred while collecting the experimental data of Mattock and Wang's[31] beam test. First, the area of compression reinforcement, which was indicated as 1570 mm^2 in the paper, should be 157 mm^2. A second error was noted where the results from five symmetrically reinforced beams were not shown in the results. The recalculations that the discusser presented in Table 12 are correct. This made the comparison between the results of shear-bending interaction formula and bending-shear-axial compression different from the results shown in the paper. The discusser recalculated the comparison result using the correct experimental data. From the discusser's Table 11, the mean of comparison result is 1.49, and the coefficient of variation is 7.9%. The average value of the comparison result is higher than 1, which means that Eq. (24) is conservative. The coefficient of variation is also very small, indicating Eq. (24) can reflect the rule of the bending-shear interaction. Herein, the authors also compared Gupta and Collins' experimental test data[40] with

Eq. (24) with a mean and coefficient of variation of 1.15 ± 16.5%, indicating Eq. (24) is reasonable to express bending-shear interaction.

The same question was posed by the discusser in the bending-shear-axial compression part. The mean of Eq. (29) will be 1.46 according to discusser's calculation, indicating that Eq. (29) is also conservative. The objective of the paper is to propose the equation form of the unified interaction formula model, and the parameters in the unified formula could be adjusted by more experimental data to fit the test data and reflect the interaction rule well. Further research should be conducted to compare more experimental data with the unified formula and make this formula more accurate and reasonable.

It is very difficult to find test components that are subjected to combined bending, shear, torsion, and axial compression. The authors considered all the Zhao's test beams to be symmetrically reinforced. If only the four symmetrically reinforced components in Table 7 are used, the mean of comparison result is 1.60 and the coefficient of variation is 4.2%. This means Eq. (35) is a little conservative but could reflect the interaction of bending, shear, torsion, and axial compression.

REFERENCES

39. Hsu, T. T. C., and Mo, Y. L., *Unified Theory of Concrete Structures*, John Wiley & Sons, Inc., New York, 2010, 518 pp.

40. Gupta, P. R., and Collins, M. P., "Evaluation of Shear Design Procedures for Reinforced Concrete Members under Axial Compression," *ACI Structural Journal*, V. 98, No. 4, July-Aug. 2001, pp. 537-547.